# Polar Enhanced Resolution Freeze/Thaw Data Record from AMSR-E and AMSR2 (Version 2.1)

**Contact Information:**

Youngwook Kim, John S. Kimball, Jinyang Du. and Tobias Kundig
Numerical Terradynamic Simulation Group (NTSG)
The University of Montana
Missoula MT, 59812

**Email**: john.kimball@umontana.edu; youngwook.kim@umontana.edu; jinyang.du@umontana.edu; tobias.kundig@umconnect.umt.edu

**Project URL**: http://freezethaw.ntsg.umt.edu/

**Release date**: 2021-08-30;
**Data record and documentation updated**: 2023-04-05

**The following reference should be used to cite these data**:

Kim, Y., J. S. Kimball, J. Du, and J. Glassy. 2022. MEaSUREs Polar Enhanced Resolution Freeze/Thaw Data Record from AMSR-E and AMSR2, Version 02 [2002 to 2021]. Boulder Colorado USA: National Snow and Ice Data Center. Digital media (https://doi.org/10.5067/WM9R9LQ2SA85).

**The following peer-reviewed citation describes FT-ESDR science algorithms, accuracy and performance:**

Kim, Y., J. S. Kimball, J. Glassy, and J. Du. (2017). An Extended Global Earth System Data Record on Daily Landscape Freeze-Thaw Determined from Satellite Passive Microwave Remote Sensing, *Earth System Science Data*, 9 (1), 133-147.

**Acknowledgements**: These data were generated through a grant from the NASA MEaSUREs (Making Earth System Data Records for Use in Research Environments) program (80NSSC18K0980). This work was conducted at the University of Montana under contract to NASA.

**Contents:**



## I. Introduction:

This document describes a Polar Enhanced Resolution (PER) data record of daily landscape Freeze/Thaw (FT) status derived at 6-km resolution from satellite passive microwave remote sensing. The PER product covers both Northern Hemisphere (NH) and Southern Hemisphere (SH) domains and is mapped to a polar earth-grid format that is well-suited for high latitude ($\geq 45^{o}$ N/S latitude) studies. The PER FT regional data record augments an existing global 25-km resolution FT Earth System Data Record (FT-ESDR) produced in a cylindrical equal-area earth grid format (Kim et al., 2017a). The FT state parameter quantifies the predominant frozen or non-frozen state of the landscape and is closely linked to changes in the surface energy budget and evapotranspiration (Kim et al., 2018a; Zhang et al. 2011), vegetation growth and phenology (Kim et al., 2014b, 2020), snowmelt dynamics (Kim et al., 2015), permafrost extent and stability (Park et al., 2016), terrestrial carbon budgets and land-atmosphere trace gas exchange (Kim et al., 2014a). Satellite microwave remote sensing is well suited for global FT monitoring due to its relative insensitivity to atmospheric contamination and solar illumination effects, and strong microwave sensitivity to changes in surface dielectric properties between frozen and non-frozen conditions.

## II. Data description

The PER FT Earth System Data Record (PER FT-ESDR) was primarily derived using similar calibrated overlapping daily [morning (AM) and afternoon (PM) overpass] radiometric brightness temperature ($T_b$) measurements at 36.5 GHz (V-pol) frequency from the NASA Advanced Microwave Scanning Radiometer for EOS (AMSR-E) and the JAXA Advanced Microwave Scanning Radiometer 2 (AMSR2) series. The latest product release (Version 2.1) includes an additional data year (2021), but with no other changes from the previous (Version 2.0) product release and associated retrieval algorithms or product format; the resulting PER FT-ESDR represents a consistent, daily FT polar record that extends over a 20 year (2002 to 2021) observation period, ensuring cross-sensor consistency through double-differencing calibration of AMSR2 to AMSR-E $T_b$ records (Du et al., 2014). Double-differencing calibration was conducted using similar frequency collocated overlapping $T_b$ records from the FY-3B Microwave Radiation Imager (MWRI), which was applied to fill the temporal $T_b$ gaps for the 2011-2012 period (Du et al., 2014). The MWRI on the Chinese FengYun 3B (FY3b) satellite was launched in November 2010 (Yang et al., 2011) and has similar instrument configuration and data acquisition times as the AMSR-E and AMSR2 (hereafter AMSR) sensors.

Calibrated $T_b$ data records from the AMSR sensors were used to develop a daily PER FT-ESDR over the NH and SH domains. The 6-km resolution of the PER FT product grid provides approximately four-fold improved spatial resolution over the global 25-km resolution FT-ESDR product and is enabled by processing of orbital swath $T_b$ retrievals closer to the native AMSR 36.5 GHz sensor footprint. The AMSR-E 36.5 GHz orbital swath $T_b$ data have a native footprint resolution of 14km x 8km (Kawanishi et al., 2003), while the similar frequency $T_b$ orbital swath (L1R) data from AMSR2 has a native 12km x 7km footprint resolution (Imaoka et al., 2010, 2012). The AMSR swath $T_b$ data were re-projected to a 6-km polar EASE-Grid 2.0 projection format (Brodzik et al., 2014) using an Inverse Distance Squared spatial interpolation approach following previously established methods (Du et al., 2017). Detailed descriptions of the FT-ESDR methods, algorithm performance and product accuracy are provided by Kim et al. (2017a).

The FT-ESDR is intended to have sufficient accuracy, resolution, and coverage to resolve physical processes linking Earth's water, energy and carbon cycles. The product is designed to determine the FT status of the composite landscape vegetation-snow-soil medium to a sufficient level to characterize the frozen temperature constraints to surface water mobility, vegetation productivity, ecosystem respiration and land-atmosphere carbon ($CO_2$) fluxes. The FT-ESDR utilizes a daily binary FT state classification on a per grid cell basis, posted to a polar 6-km Earth grid. The 6-km polar projection format provides enhanced FT spatial grid resolution closer to the native footprint of the 36.5 GHz AMSR $T_b$ retrievals, and with less spatial distortion over the polar regions relative to the global FT-ESDR product. The FT classification algorithm uses a temporal change detection of radiometric $T_b$ time-series that identify FT transition sequences by exploiting the dynamic temporal $T_b$ response to differences in the aggregate landscape dielectric constant that occur as the landscape transitions between predominantly frozen and non-frozen conditions (McDonald and Kimball 2005; Kim et al., 2011, 2012). AMSR ascending and descending orbital $T_b$ time series are processed separately to produce information on morning (0130 AM), afternoon (1330 PM) and composite daily FT conditions (CO). Additional variables distinguished by the FT-ESDR include transitional (AM frozen and PM thawed) or inverse transitional (AM thawed and PM frozen) conditions. **Table 1** describes the file encoding of FT-ESDR pixel values corresponding to frozen, thawed, and transitional conditions. The PER FT-ESDR domain encompasses all NH and SH land areas affected by seasonal frozen temperatures, including urban, barren land, snow-ice and open water body dominant grid cells (Kim et al., 2017a).

**Table 1**. FT-ESDR 8-bit integer data identifiers.

| Classification | FT DN |
|---|---|
| Frozen (AM/PM frozen) | 0 |
| Thawed (AM/PM thawed) | 1 |
| Transitional (AM frozen and PM thawed) | 2 |
| Inverse Transitional (PM frozen and AM thawed) | 3 |
| No FT status available | 252 |

| | |
|---|---|
| Non-cold constraint area | 253 |
| 100% open water | 254 |
| Fill value | 255 |

Both PER and global FT-ESDR data records are available for public access via FTP download through the FT-ESDR project web site (http://freezethaw.ntsg.umt.edu) and NTSG HTTP Data Service (http://files.ntsg.umt.edu/data/FT_ESDR_PER/), and through the NASA DAAC at the National Snow and Ice Data Center (https://nsidc.org/data/nsidc-0728); these data include a variety of file formats including Geotiff and searchable metadata. The FT-ESDR is projected in a polar cylindrical Equal-Area Scalable Earth (EASE) grid, Version 2 format (Brodzik et al., 2014) consistent with the format of the underlying AMSR polar $T_b$ records used as primary inputs for the FT classification.

## III. PER FT-ESDR version 2 protocols and changes from prior releases

The Version 2 (v2.1) PER product contains similar protocols used to construct the baseline global FT-ESDR version 5.0 product and previous PER FT-ESDR (v1.0) product (Kim et el. 2017a, 2018b). The current Version 2 PER product replaces previous PER product versions. The following summarizes the latest PER product version (v2.1) upgrades:

- A long-term FT data record is represented, extending over the combined calibrated AMSR (AMSR-E and AMSR2) period of record from 2002 to 2021 (~20 years);
- The PER FT-ESDR includes both Northern Hemisphere (NH) and Southern Hemisphere (SH) polar grid domains to facilitate high latitude studies of the changing cryosphere in both polar hemispheres;
- A modified seasonal threshold algorithm (MSTA) is used for the FT classification where MSTA $T_b$ reference FT conditions are calibrated annually for each pixel using 6-km resolution daily surface air temperature (SAT) records downscaled from coarser resolution (0.25°) ERA5 reanalysis data (Hersbach et al., 2018) using temperature lapse rates defined from an Aqua MODIS LST climatology and digital elevation map;
- Over NH permanent snow/ice regions, an Adaptive Threshold algorithm (ADT) is used by adaptively determining the FT threshold from analyzing $T_b$ time series of a

given year and grid cell (Kimball et al., 2021). For areas where seasonal melting events occur, a Breaks For Additive Seasonal and Trend (BFAST) approach (Verbesselt et al., 2012) is applied to detect the abrupt change point connecting the adjacent frozen and thawed periods to determine FT reference $T_b$ values. For areas where there is no persistent snow/ice melting, diurnal change signals from AMSR ascending and descending orbit Tb retrievals are used to confirm diurnal thaw and refreeze events and determine FT reference Tb values;

- Updated annual data quality assurance (QA) maps are included indicating product performance and reliability.

Differences from the baseline global FT-ESDR data include finer spatial resolution (6 km) FT daily data records and polar EASE-grid 2.0 format, which reduces spatial distortion of FT grid cells at higher (N/S) latitudes relative to the FT-ESDR global grid product.

## IV. FT-ESDR accuracy and performance

The Version 2 PER FT-ESDR is developed by merging AMSR-E and AMSR2 36.5 GHz frequency, vertical (V) polarization $T_b$ records, and applying similar protocols used to construct earlier PER FT-ESDR product versions (Kim et el. 2018b). The PER FT-ESDR has been verified against a range of other independent FT metrics, including daily surface air temperature (SAT) records from NH and SH weather stations (Kim et al., 2017a). The FT-ESDR product accuracy is primarily assessed in relation to daily SAT maximum ($SAT_{max}$) and minimum ($SAT_{min}$) values from the WMO weather station network (4718±901 [temporal-SD] stations for NH domain and 352±31 [temporal-SD] stations for SH domain). Daily $SAT_{min}$ and $SAT_{max}$ records for the selected stations were used to define daily frozen (SAT ≤ 0 °C) and non-frozen (SAT >0 °C) states and compare with the respective AM and PM FT-ESDR products. The FT classification agreement was assessed through grid-cell-to-point comparisons between WMO daily SAT measurements and overlying FT-ESDR results (Kim et al., 2017). Mean annual FT spatial classification accuracies are approximately 93.2±0.5 [inter-annual SD] and 86.5±0.8 [inter-annual SD] percent for respective PER FT PM and AM retrievals over the NH domain and long-term record. The SH mean annual FT spatial classification accuracies are approximately 99.0±0.2 [inter-annual SD] and 92.4±1.1 [inter-annual SD] percent for respective PM and AM

retrievals. The PER FT classification accuracy shows strong seasonal and annual variability, and is generally lower during active FT transition periods when spatial heterogeneity in landscape FT processes is maximized (Kim et al. 2017a). Daily FT spatial classification accuracy is defined for each product daily granule from pixel-wise comparisons of FT classification accuracy in relation to co-located weather station network daily air temperature ($SAT_{min}$, $SAT_{max}$) measurements (Kim et al. 2017a); spatial classification accuracy is expressed as the proportion of stations where the daily FT classification is consistent with station SAT measurement based FT estimates. Other data quality (QA) metrics are included that provide more spatially explicit information on algorithm performance, including potential negative impacts from open water cover, terrain complexity, length of FT transitional season, and MSTA FT threshold uncertainty influencing mean annual classification accuracy.

**V. FT algorithms:**

The PER FT-ESDR classification involves a modified seasonal threshold algorithm (MSTA) approach with radiometric $T_b$ time-series that identify FT transition sequences by exploiting the dynamic $T_b$ temporal response to differences in the aggregate landscape dielectric constant that occur as the landscape transitions between predominantly frozen and non-frozen conditions. The PER FT-ESDR classification over NH permanent snow/ice regions (e.g., Greenland) adopts an Adaptive Threshold algorithm (ADT), which involves BFAST and diurnal change FT detection for respective areas with and without persistent seasonal melting (Kimball et al., 2021). These techniques are well-suited for resolving daily FT state dynamics rather than single events or seasonally dominant transitions (Kim et al. 2011, 2017a; Kimball et al., 2021). The Version 2 product uses the MSTA and ADT to classify daily (AM and PM) FT status from 36.5 GHz (V-pol) $T_b$ time series from the AMSR records. The MSTA FT threshold established for each grid cell is defined annually using an empirical linear regression relationship between the satellite $T_b$ retrievals and daily 6-km SAT downscaled from coarser (0.25 degree) spatial resolution ERA5 (Hersbach et al., 2018) global reanalysis daily surface temperature data using a digital elevation map (DEM: Hasting et al., 1999) and an annual mean environmental lapse rate (ELR). The daily grid cell-wise ELR was derived from the linear regression relationship between DEM elevations and MODIS Aqua land surface temperature (LST) retrievals (Kim et al., 2017b). The FT

thresholds were derived separately for the satellite $T_b$ time series from AM and PM overpasses and using corresponding daily SAT minimum ($SAT_{min}$) and maximum ($SAT_{max}$) values. Larger weighting of SAT values closer to 0°C was used in selecting the corresponding $T_b$ based FT threshold for each grid cell; weighting of the SAT and $T_b$ regression relationship was derived using a cosine function within a temperature range extending from -60.0°C to 30.0°C and representing 99 percent of the SAT frequency distribution defined from the 36-year SAT global climatology (Kim et al., 2017a). An advantage of the MSTA relative to an earlier seasonal threshold algorithm (STA) based FT classification (Kim et al. 2011) is that the $T_b$ threshold selection does not depend on frozen and non-frozen reference states derived by averaging $T_b$ measurements over respective winter and summer periods, and is less sensitive to $T_b$ data gaps during these reference periods. Similar to the MSTA, the ADT algorithm is also a threshold-based approach but is adapted for more predominant snow/ice areas. For these areas, the snow/ice melting period is generally characterized by higher $T_b$ values relative to the frozen period; and large $T_b$ diurnal variability may suggest snow microstructure changes from thaw and refreeze events. Accordingly, an advantage of the ADT is that no ancillary data are required for FT detection and the threshold values are determined directly from the breaks in seasonal $T_b$ trends and diurnal $T_b$ variability (Kimball et al., 2021).

**VI. Ancillary data used for the FT-ESDR**

We used daily SAT records from ERA5 model reanalysis for pixel-wise annual calibration the MSTA FT thresholds. The reanalysis data were also used to define the polar FT-ESDR domain (**Figure 1**) using a simple SAT driven bioclimatic index (Kim et al. 2011) that identified all land areas where seasonally frozen air temperatures are a significant constraint to ecosystem processes and land surface water mobility (Kim et al., 2017a).

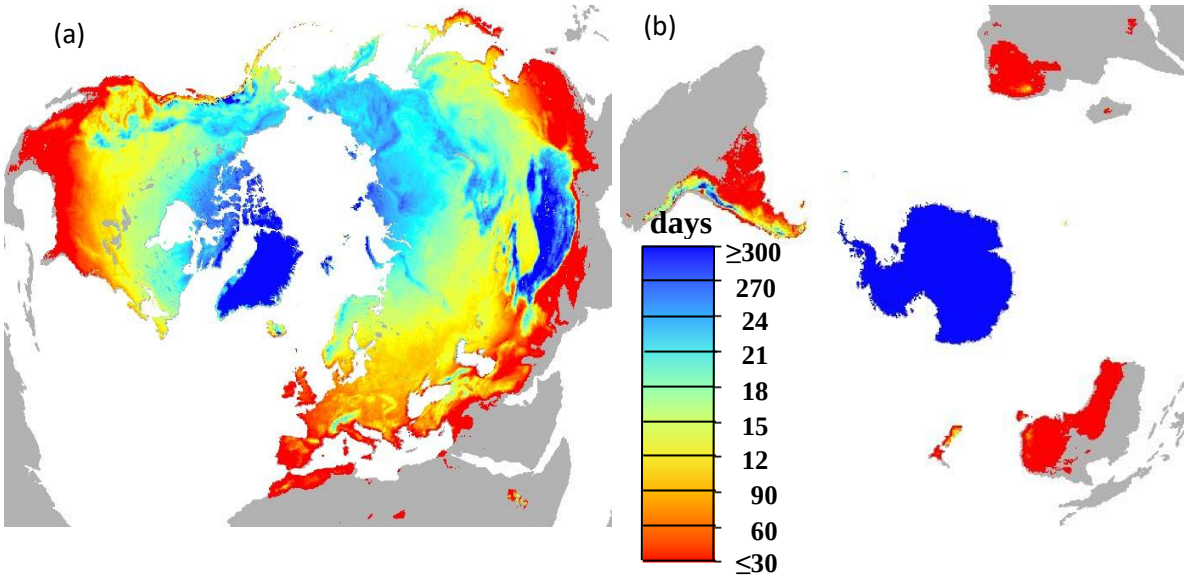


***Figure 1****: PER FT-ESDR derived mean annual frozen season (frozen or transitional status) over the NH (a) and SH (b) domains; white and grey colors denote respective open water bodies and land areas outside of the FT-ESDR domain.*

Independent daily SAT observations from in situ WMO weather station measurements were used for verification of FT-ESDR daily accuracy. A simple zero degree Celsius temperature threshold was used to classify frozen and non-frozen temperatures from the SAT measurements; these results were then compared against the FT-ESDR daily classification results from the overlying grid cell. The resulting FT spatial classification accuracy from all WMO stations was then summarized on a daily basis.

A polar QA map is defined for each year of record and provides a discrete, grid cell-wise indicator of relative FT-ESDR quality that accounts for potential negative impacts from open water cover, terrain complexity, length of FT transitional season, and MSTA FT threshold uncertainty influencing mean annual FT classification accuracy indicated from the WMO station comparisons. The resulting annual QA map for selected year 2012 is presented in **Figure 2** and shows regions of relative high to low quality. The QA values were stratified into a smaller set of

discrete categories ranging from low (estimated mean annual FT classification accuracy < 70%) to best (> 90%) quality. Mean proportions of the four QA categories encompass 68.7% (best), 24.6% (good; 80-90% agreement), 4.3% (moderate; 70-80% agreement), and 2.4% (low; <70% agreement) of the polar FT-ESDR domain for the NH domain. For the SH domain, mean QA proportions include 80.3% for best category, 14.8% for good category, 3.5% for moderate category, and 1.5% for low category results.

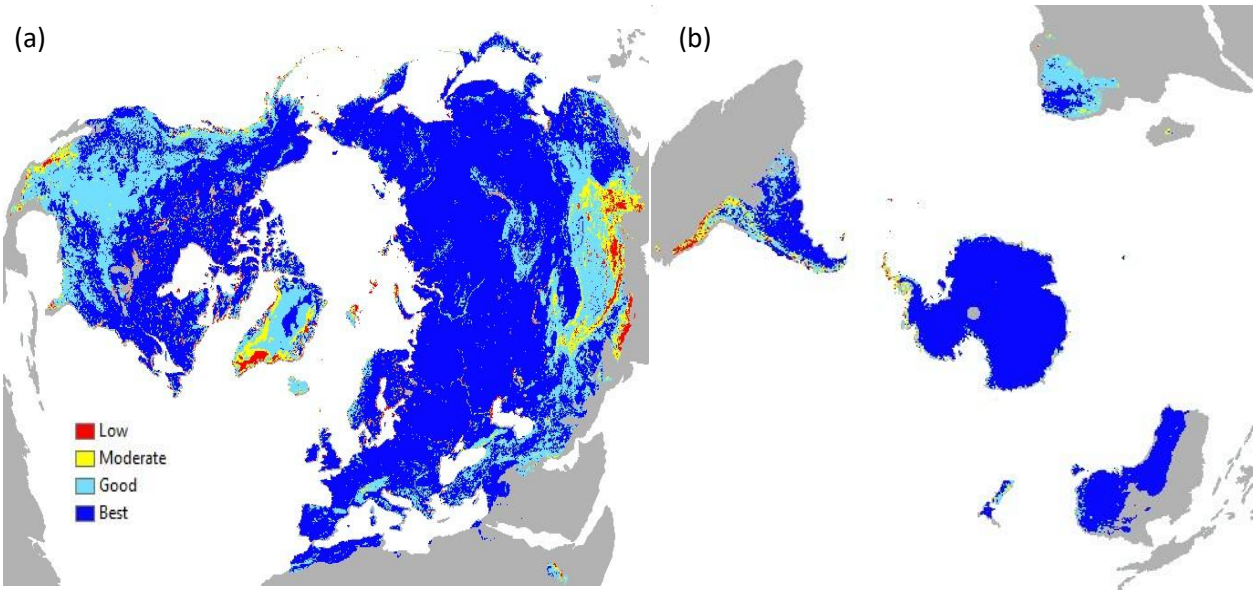


***Figure 2****: FT-ESDR annual quality assurance (QA) map for 2012, and over the NH (a) and SH (b), aggregated into low (estimated mean annual spatial classification agreement < 70%), moderate (70-80%), good (80-90%) and best (>90%) relative quality categories. Land areas outside of the FT-ESDR domain are denoted by grey shading.*

**VII. Hierarchical data archive structure and available software tools:**

The University of Montana FT-ESDR data are publicly accessible through the online NTSG FTP service. The PER data are organized in a hierarchical file structure by geographic domain (NH and SH) and year of record. The PER v2 data and associated file structure are also available in a set of compressed "tar" archive files to facilitate downloading of the complete record. The tar archives consist of the following files as documented in **Table 2** below. The data includes daily FT classification files in GeoTIFF format; daily FT accuracy and annual QA maps, and supporting FT-ESDR documentation and software tools.

**Table 2**. Tar archive files encompassing the PER FT-ESDR (v2) product release.

| PER FT-ESDR v2.0 File Summary | |
|---|---|
| [1]Directory | Summary of Contents |
| DAILY_ BINARY | Multi-year record of polar daily binary granules |
| QA_ACCURACY | Daily FT-ESDR mean polar classification accuracy (%) and annual QA metadata in GeoTIFF file format. Value -9999 refers to no data. |
| TAR_ARCHIVES | Compressed tar files (*.tar.gz) FT gridded (global EASE-grid) data files archive for distribution and network transfer |
| MD5 | MD5 checksum hash signatures for each FT file in the collection |
| DOC | FT-ESDR database documentation files |

*[1]Note that within a given directory tree such as DAILY_GEOTIFF , there is a sub-tree for a series of year-wise directories (2002-2021).*

Commonly available software tools routinely used with the GeoTIFF file formats this PER distribution is produced in include ArcGIS, IDL/ENVI, MatLAB, "R", and various Python implementations that support user developed code.

## VIII. Data format and file naming convention:

### Daily FT Status

Each FT-ESDR grid cell is projected in a polar EASE-Grid 2.0 format (Brodzik et al., 2014) at 6-km spatial resolution, with 3000 columns and 3000 rows consisting of 8-bit byte data type, for a total of 9000000 pixels per daily data product. An ESRI projection file is included with the GeoTIFF files to aid in viewing the data in the ArcMap and ArcGIS software environment. The geographical range of the PER product extends from -179.9999° to 179.9999° longitude and from 0° to 90.0° N/S latitude covering both NH and SH polar domains.

Each daily FT file consists of 3 separate granules, including: morning overpass (AM), afternoon overpass (PM) and combined daily AM and PM (CO) classification results. The FT product file naming protocol follows these conventions:

[InstrumentLabel]_[Channel][Polarization]_[OverpassCode]_FT_[Year]_day[DOY]_[Hemisphere]_06km. [FileExtension]

For example, the binary file "AMSR_36V_CO_FT_2016_day365_NH_06km.bin" represents AMSR sensor, 36.5 GHz, vertically polarized $T_b$ based FT classification for composite daily conditions for day (calendar year) 365 over the NH domain and at 6-km spatial resolution.

**Annual FT Accuracy**

Annual accuracy files are available for both AM and PM overpasses. Relative accuracy is assessed in relation to daily maximum and minimum air temperature (SAT) measurements from the global WMO weather station network and expressed as the percent of satellite derived daily FT retrievals per year that are consistent with independent in situ FT observations derived from WMO SAT measurements. Values are reported in the range from 0.0 to 100.0 percent. The accuracy file naming protocol follows these conventions:

[InstrumentLabel]_[Channel][Polarization]_[OverpassCode]_FT_[Year]_accuracy_[Hemisphere]_06km_EASE2.bin

**Annual FT Quality Assurance**

The annual FT Quality Assurance (QA) metric represents a relative index of data quality for each grid cell based on the potential negative impacts imposed from various conditions (Kim et al. 2017), including $T_b$ data gaps, open water, terrain complexity, length of FT transitional season, and uncertainty in the FT algorithm threshold. QA values are reported from 0.0 to 1.0 and categorized as: QA < 0.70 = low; 0.70 < QA < 0.85 = moderate; 0.85 < QA < 0.95 = good; and QA > 0.95 = best quality indicators. Separate files are available for each calendar year in each satellite record. The QA file naming protocol follows these conventions:

[InstrumentLabel]_ [Hemisphere]_QA_[Year]_[OverpassCode].[FileExtension]

**IX. Data Organization and Volume:**

The daily FT data is organized in this collection first by sensor label, and then by year, with the AM, PM and CO granules stored in each annual directory. Both the Northern and Southern hemisphere PER file sizes are listed in (**Table 3**). In addition to the primary FT data, detailed product quality information is also provided that includes granule level total mean spatial classification accuracy for the NH and SH domains defined on a daily basis (defined from pixel-

wise comparisons against co-located global weather station SAT observations), and spatially contiguous relative data quality (QA) maps updated for each annual cycle. The PER FT-ESDR consists of a total of 19526 daily NH 6km resolution granules, for a total of 168 Gb (Geotiff form) for the entire hemispheric FT record. The SH portion of the FT record consists of 19525 6km granules, for a total of 165 Gb for the entire hemispheric data record. The entire global PER record (both NH and SH components) represents a total storage volume of 333 Gb. For faster downloading, compressed ("gzip") yearly FT binary files are provided in the "DAILY_TAR_ARCHIVES" directory.

**Table 3**. FT-ESDR file size summaries for Geotiff files.

| Instrument | N. files | Range of Years | GeoTiff Files |
|---|---|---|---|
| AMSR-E and AMSR2 (NH) | 19853 | 2002 – 2021 | 170 Gb |
| AMSR-E and AMSR2 (SH) | 19853 | 2002-2021 | 167 Gb |

A number of compressed tar archives (**Table 4**) are also available (see DAILY_TAR_ARCHIVES directory) as a convenient method for users to access related collections of the FT- ESDR files. Their names, manifests (table of content files), number of files, and data volume sizes are documented in the table below:

**Table 4**. FT-ESDR compressed tar file (tar.gz) archives and file sizes available for download.

| Tar Archive Name | N. Files | Size |
|---|---|---|
| FT_V2_NH_AMSR_GeoTIFF.tar.gz | 19853 | 7.4 Gb |
| FT_V2_NH_ANNUAL_QA.tar.gz | 80 | 256 Mb |
| FT_V2_NH_AMSR_Binary.tar.gz | 20583 | 3.7 Gb |
| FT_V2_SH_AMSR_GeoTIFF.tar.gz | 19853 | 2.1 Gb |
| FT_V2_SH_AMSR_Binary.tar.gz | 20583 | 1.9 Gb |
| FT_V2_SH_ANNUAL_QA.tar.gz | 80 | 90 Mb |

**X. Example FT Figures:**

The FT-ESDR provides a daily (CO) classification of the predominant landscape frozen or non-frozen status for each grid cell within the NH and SH domains (**Figure 3, 4**). Four discrete FT metrics are distinguished from the AM and PM $T_b$ retrievals, including frozen (both AM and PM overpasses), non-frozen (AM and PM), transitional (AM frozen, PM non-frozen) and inverse-transitional (AM non-frozen, PM frozen) states.

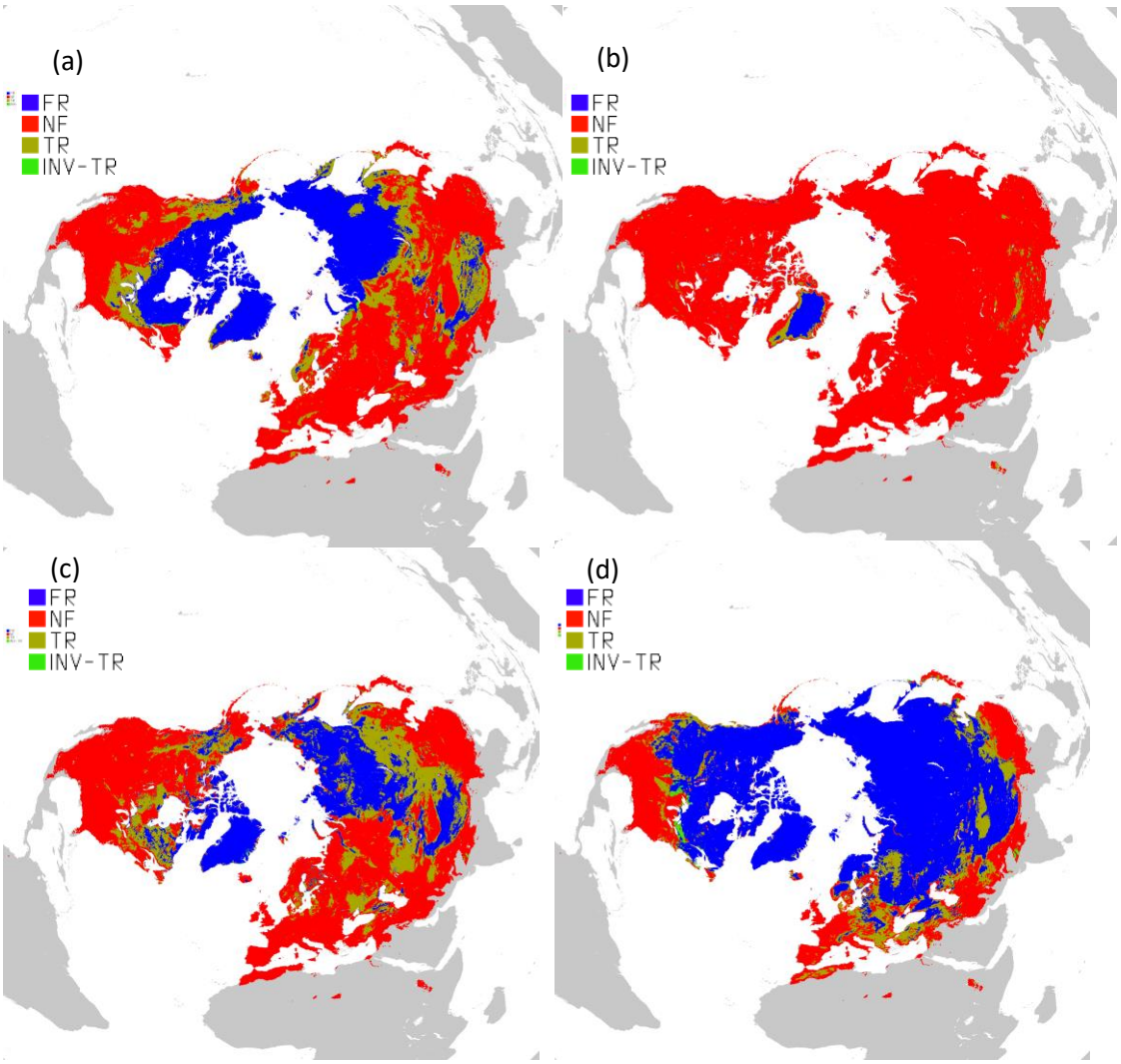


***Figure 3**: Daily combined (CO) NH FT-ESDR classification results from selected year of record 2016, where: (a) DOY (Day of Year) =100, (b) DOY=200, (c) DOY=300, and (d) DOY=360; white and grey colors denote respective open water bodies and land areas outside of the FT-ESDR domain; FR (AM and PM frozen), NF (AM and PM thawed), TR (AM frozen and PM thawed) and INV-TR (AM thawed and PM frozen).*

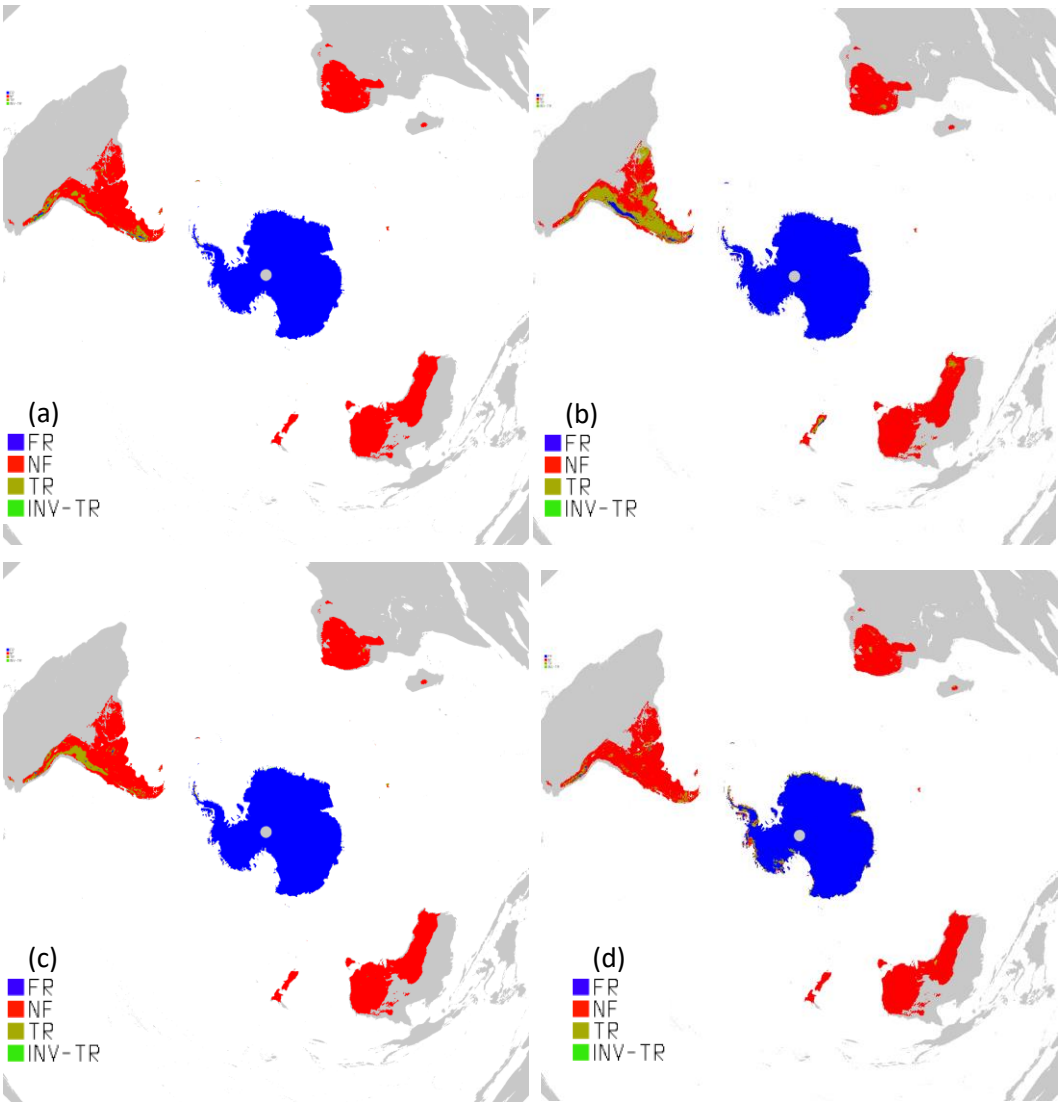


***Figure 4****: Daily combined (CO) SH FT-ESDR classification results from selected year of record 2016, where: (a) DOY (Day of Year) =100, (b) DOY=200, (c) DOY=300, and (d) DOY=360; white and grey colors denote respective open water bodies and land areas outside of the FT-ESDR domain; FR (AM and PM frozen), NF (AM and PM thawed), TR (AM frozen and PM thawed) and INV-TR (AM thawed and PM frozen).*

**XI. References:**


Armstrong, R. L. and M. J. Brodzik. 1995. An Earth-Gridded SSM/I Data Set for Cryosphere Studies and Global Change Monitoring. *Advances in Space Research*. 16, 155-163.

Armstrong, R., K. Knowles, M. Brodzik, and M.A. Hardman, 1998, updated 2012. DMSP SSM/I-SSMIS Pathfinder Daily EASE-Grid Brightness Temperatures. Version 2 [1987-2012]. Boulder, Colorado USA: NASA DAAC at the National Snow and Ice Data Center (http://nsidc.org/data/nsidc-0032.html).

Brodzik, M. J., B. Billingsley, T. Haran, B. Raup and M. H. Savorie. 2014. Correction: Brodzik, M. J. et al. EASE-Grid 2.0: Incremental but significant improvements for Earth-Gridded Data sets. *ISPRS International Journal of Geo-Information*, 3 (3), 1154-1156

Brodzik, M. J. and R. L. Armstrong. 2002. EASE-Grid: A versatile set of equal-area projections and grids. In M. Goodchild (Ed.), Discrete Global Girds. Santa Barbara, California USA: National Center for Geographic Information and Analysis.

Du, J., J. S. Kimball, C. Duguay, Y. Kim, and J. D. Watts. 2017. Satellite microwave assessment of Northern Hemisphere lake ice phenology from 2002 to 2015. *The Cryosphere*, 11, 47-63

Du, J., J. S. Kimball, and L. Jones. 2015. Satellite Microwave Retrieval of Total Precipitable Water Vapor and Surface Air Temperature Over Land from AMSR2. *IEEE Transactions on Geoscience and Remote Sensing*, 53 (5), 2520-2531

Du, J., J. S. Kimball, J. Shi, L. A. Jones, S. Wu, R. Sun, and H. Yang. 2014. Inter-calibration of satellite passive microwave land observations from AMSR-E and AMSR2 using overlapping FY3B-MWRI sensor measurements. *Remote Sensing*, 6, 8594-8616

Ferraro, R. R., F. Weng, N. C. Grody, and A. Basist. 1996. An eight-year (1987-1994) time series of rainfall, clouds, water vapor, snow cover, and sea ice derived from SSM/I measurements. *Bulletin of the American Meteorological Society*, 77(5), 891-905

Friedl, M. A., D. K. McIver, J. C. F. Hodges, X. Y. Zhang, D. Muchoney, A. H. Strahler, C. E. Woodcock, S. Gopal, A. Schneider, A. Cooper, A. Baccini, F. Gao, and C. Schaaf. 2002. Global land cover mapping from MODIS: algorithms and early results. *Remote Sensing of Environment*, 83, 287-302

GLOBE Task Team and others (Hasting, D. A., P. K. Dunbar, G. M. Elphingstone et al. 1999. The global land one-kilometer base elevation (GLOBE) digital elevation model, version 1.0. National Oceanic and Atmospheric Administration, National Geophysical Data Center, 325 Broadway, Boulder, Colorado 80305-3328, U.S.A. Digital data base on the World Wide Web (http://www.ngdc.noaa.gov/mgg/toto/globe.html) and CD-ROMs.

Hersbach, H., Bell, B., Berrisford, P., Biavati, G., Horányi, A., Muñoz Sabater, J., Nicolas, J., Peubey, C., Radu, R., Rozum, I., Schepers, D., Simmons, A., Soci, C., Dee, D., Thépaut, J-N. 2018. ERA5 hourly data on single levels from 1979 to present. Copernicus Climate Change Service (C3S) Climate Data Store (CDS).

Imaoka, K.; Takashi, M.; Misako, K.; Marehito, K.; Norimasa, I.; Keizo, N. 2012. Status of AMSR2 instrument on GCOM-W1, earth observing missions and sensors: Development, implementation, and characterization II. Proc. SPIE 2012, 852815, doi:10.1117/12.977774

Imaoka, K., M. Kachi, M. Kasahara, N. Ito, K. Nakagawa, and T. Oki. 2010. Instrument performance and calibration of AMSR-E and AMSR2, ISPRS Archives, 38 (8), 13-18

JAXA. Digital media (https://gcom-w1.jaxa.jp).

Jones, L.A., and J.S. Kimball, 2010, updated 2012. Daily Global Land Surface Parameters Derived from AMSR-E, Version 1.1. Boulder Colorado USA: National Snow and Ice Data Center. Digital media (http://nsidc.org/data/nsidc-0451.html).

Kawanishi, T. J., T. Sezai, Y. Ito, K. Imaoka, T. Takashima, Y. Ishido, A. Shibata, M. Miura, H. Inahata, and R. W. Spencer. (2003). The advanced scanning microwave radiometer for the EarthObserving System (AMSR-E): NASDA's contribution to the EOS for global energy and water cycle studies. *IEEE Transactions on Geoscience and Remote Sensing*, 41 (2), 184-194

Kim Y., Kimball J.S., Parazoo N., Kirchner P. 2020. Diagnosing Environmental Controls on Vegetation Greening and Browning Trends Over Alaska and Northwest Canada Using Complementary Satellite Observations. In: Yang D., Kane D. (eds) Arctic Hydrology, Permafrost and Ecosystems. Springer, doi.org/10.1007/978-3-030-50930-9_20

Kim, Y., J. S. Kimball, J. Du, C. L. B. Schaaf, and P. B. Kirchner. 2018a. Quantifying the effects of freeze-thaw transitions and snowpack melt on land surface albedo and energy exchange over Alaska and Western Canada, Environmental Research Letters, 13 (7), 1-14

Kim, Y., J. S. Kimball, J. Glassy, and K. C. McDonald. 2018b, updated 2019. MEaSUREs Northern Hemisphere Polar EASE-Grid 2.0 Daily 6 km Land Freeze/Thaw Status from AMSR-E and AMSR2, Version 1. [Indicate subset used]. Boulder, Colorado USA. NASA National Snow and Ice Data Center Distributed Active Archive Center. doi: https://doi.org/10.5067/WM9R9LQ2SA85.

Kim, Y., J. S. Kimball, J. Glassy, and J. Du. 2017a. An Extended Global Earth System Data Record on Daily Landscape Freeeze-Thaw Determined from Satellite Passive Microwave Remote Sensing, *Earth System Science Data*, 9 (1), 133-147

Kim, Y., J.S. Kimball, & J. Du. 2017b. Chapter 8. Satellite microwave remote sensing of landscape freeze-thaw status related to frost hazard monitoring . *Remote Sensing of Hydro-Meteorological Hazards* (Boca Raton, FL: CRC Press).

Kim, Y., J. S. Kimball, D. A. Robinson, and C. Derksen. 2015. New satellite climate data records indicate strong coupling between recent frozen season changes and snow cover over high northern latitudes. *Environmental Research Letters*, 10, 084004.

Kim, Y., J. S. Kimball, K. Zhang, K. Didan, I. Velicogna, and K. C. McDonald. 2014a. Attribution of divergent northern vegetation growth responses to lengthening non-frozen seasons using satellite optical-NIR and microwave remote sensing, *International Journal of Remote Sensing*, 10.1080/01431161.2014.915595

Kim, Y., J. S. Kimball, K. Didan, and G. M. Henebry. 2014b. Responses of vegetation growth and productivity to spring climate indicators in the conterminous Unites States derived from satellite remote sensing data fusion. *Agricultural and Forest Meteorology*, 194, 132-143

Kim, Y., J.S. Kimball, K. Zhang, and K.C. McDonald, 2012. Satellite detection of increasing northern hemisphere non-frozen seasons from 1979 to 2008: Implications for regional vegetation growth. *Remote Sensing of Environment* 121, 472-487.

Kim, Y., J. S. Kimball, K. C. McDonald, and J. Glassy. 2011. Developing a Global Data Record of Daily Landscape Freeze/Thaw Status using Satellite Microwave Remote Sensing. *IEEE Transactions on Geoscience and Remote Sensing.* 49, 3, 949-960.

Kimball, J.S., Du, J., Meierbachtol, T.W., Kim, Y. and Johnson, J.V. (2021). Comparing Greenland Ice Sheet Melt Variability From Different Satellite Passive Microwave Remote Sensing Products Over a Common 5-year Record. *Front. Earth Sci*, 9, p.654220.

Knowles, K., M. Savoie, R. Armstrong, and M. Brodzik, 2006, updated 2011. AMSR-E/Aqua Daily EASE-Grid Brightness Temperatures [2002-2011]. Boulder, Colorado USA: NASA DAAC at the National Snow and Ice Data Center (http://nsidc.org/data/nsidc-0301.html).

Knowles, K., E.G. Njoku, R. Armstrong, and M. Brodzik, 2000. Nimbus-7 SMMR Pathfinder Daily EASE-Grid Brightness Temperatures [1979-1987]. Boulder, Colorado USA: NASA DAAC at the National Snow and Ice Data Center (http://nsidc.org/data/nsidc-0071.html).

McDonald, K.C, and J.S. Kimball, 2005. Hydrological application of remote sensing: Freeze-thaw states using both active and passive microwave sensors. Encyclopedia of Hydrological Sciences. Part 5. Remote Sensing. M.G. Anderson and J.J. McDonnell (Eds.), John Wiley & Sons Ltd. DOI:10.1002/0470848944.hsa059a.

Park, H., Y. Kim, and J. S. Kimball. (2016). Widespread permafrost vulnerability and soil active layer increases over the high northern latitudes inferred from satellite remote sensing and process model assessments. *Remote Sensing of Environment*, 175, 349-358.

Verbesselt, J., Zeileis, A., and Herold, M. (2012). Near real-time disturbance detection using satellite image time series. *Remote Sens. Environ*. 123, 98–108. doi:10.1016/j.rse.2012.02.022.

Yang, H., F. Weng, L. Lv, N. Lu, G. Liu, M. Bai, Q. Qian, J. He, H. Xu. 2011. The FengYun-3 microwave radiation imager on-orbit verification. *IEEE Transactions on Geoscience and Remote Sensing*, 49, 4552–4560.

Zhang, K., J.S. Kimball, Y. Kim, and K.C. McDonald, 2011. Changing freeze-thaw seasons in northern high latitudes and associated influences on evapotranspiration. *Hydrological Processes* 25, 4142-4151, DOI:10.1002/hyp.8350.